Pulmonary Architecture in the Conducting Regions of Six Rats

DONGYOUB LEE,[1]* MICHELLE V. FANUCCHI,[2] CHARLES G. PLOPPER,[2] JENNIFER FUNG,[3] AND ANTHONY S. WEXLER[1,4,5]

[1]Department of Mechanical and Aeronautical Engineering, University of California, Davis, California
[2]Department of Anatomy, Physiology, and Cell Biology, University of California, Davis, California
[3]Center For Molecular and Genomic Imaging, University of California, Davis, California
[4]Department of Civil and Environmental Engineering, University of California, Davis, California
[5]Department of Land, Air and Water Resources, University of California, Davis, California

ABSTRACT

Rats are widely used for studies of pulmonary toxicology and lung disease. Several studies suggest nominal geometric parameters describing the architecture of the rat airway. However, intersubject variance has never been reported due to the huge effort and time to take these manual measurements. In this study, we present statistics of the branching pattern of six healthy male Sprague Dawley rats by automatically analyzing computed tomography images of silicon casts of their airways. Details of branching characteristics and also intersubject variance are presented. In addition, this study shows that mean and standard deviation of many geometric parameters insufficiently represent pulmonary architecture because some, such as diameter-asymmetry, are not normally distributed. Detailed statistics including inter- and intrasubject variance and distribution of the geometric parameters will aid in constructing more realistic airway models for particle transport and studies of normal and abnormal respiratory physiology. Anat Rec, 291:916–926, 2008. © 2008 Wiley-Liss, Inc.

Key words: pulmonary architecture; Sprague Dawley rats; CT image; geometric parameter distribution

Air pollutants are known to be associated with adverse airway reactions ranging from shortness of breath to death (Dockery and Pope, 1994; Holgate et al., 1999). Studies suggest that chronic exposure during development leads to functional impairment in humans and physiological changes in animal models (Gauderman et al., 2000; Mariassy et al., 1989, 1990).

Rats are widely used for the studies of pulmonary toxicology and various models of lung architecture have been developed based on manual airway measurements (Raabe et al., 1976; Yeh et al., 1979; Phillips and Kaye, 1995). However, such anatomical studies are limited by their huge costs so that only one or at most a few subjects are studied.

Recent advances in computer technology and biomedical engineering have led to development of better medical imaging equipment capable of acquiring higher resolution images in less time than previously possible. The acquisition of large volumetric image data sets presents an opportunity to quantitatively analyze the imaging data with a potential to glean important research or clinical information not possible with qualitative examination of serial two-dimensional (2D) images or by manual measurement of casts. Several studies computerized

Grant sponsor: United States Environmental Protection Agency; Grant number: RD-83241401-0.

*Correspondence to: DongYoub Lee, Address: Mechanical and Aeronautical Engineering, One Shields Avenue, University of California, Davis, CA 95616; Fax: 530-754-4962.
E-mail: dole@ucdavis.edu

Received 3 September 2007; Accepted 7 April 2008
DOI 10.1002/ar.20726
Published online 16 June 2008 in Wiley InterScience (www.interscience.wiley.com).

© 2008 WILEY-LISS, INC.

the 3D data analysis process showing that a quantitative comparison of many airways is possible (Sera et al., 2003; Tawhai et al., 2004).

In this study, branching patterns of conducting airways of six healthy male Sprague Dawley rats were analyzed using a new computerized analysis of lung cast computed tomography (CT) images. The new analysis method fits a general bifurcation model to the CT data using an optimization method, thereby identifying detailed geometric characteristics of the airways and the error in this identification, all of which are reported here. Furthermore, we show that the distribution of rotation angle and diameter asymmetry must be taken into account to properly generate pulmonary architecture because those parameters are far from normal distribution.

MATERIALS AND METHODS

Preparation of Airway Cast

Specific pathogen-free male Sprague Dawley rats were obtained from Harlan (San Diego, CA). Animals were shipped in filtered containers and housed in laminar flow hoods in American Association for the Accreditation of Laboratory Animal Care (AAALAC) approved animal facilities with free access to food and water. Rats were kept in the University of California, Davis, animal facilities for at least 1 week before use. Table 1(a) summarizes rat and airway data for the animals used in this study and that of Raabe et al. (1976).

Animals were weighed, then anesthetized with an overdose of 12% pentobarbital and killed by exsanguination of the vena cava. The trachea was exposed and cannulated at the crico-tracheal junction. The diaphragm was punctured, collapsing the lungs, and the lungs were infused with fixative (1% glutaraldehyde/1% paraformaldehyde in cacodylate buffer, pH 7.4, 330 mOsm) at 30 cm water pressure for at least 1 hr inside the chest cavity. The trachea was ligated, and the lungs, with the cannula still attached, were removed from the cavity and stored in the same fixative at 4°C. The casting process began by removing the lungs from the fixative and washing them in phosphate buffered saline (PBS). All the lungs for this study were cast within 1 day of being killed and fixed. Lungs, attached by the cannula, were put inside a negative pressure chamber. The casting apparatus and silicone casting mixture were modified from the procedure of Perry et al. (2000). The negative pressure chamber was depressurized to −100 mm Hg. The silicone solution was made using 100% silicone rubber RTV Sealant (734 Flowable Sealant) and dimethylpolysiloxane 200 Fluid, 20 cs viscosity, both purchased from Dow Corning (Midland, MI). Varying amounts of glacial acetic acid (up to 15%) were added to decrease the silicone viscosity to aid in casting small diameter airways. The silicone mixture was added through the cannula and administered into the airways by means of vacuum pressure for 2 to 10 min depending on the size of the lung and the viscosity of the mixture. According to Perry et al. (2000), silicone sealant 734 RTV diluted with low viscosity silicone oil penetrates well to the level of the respiratory bronchioles and alveolar ducts without causing overdistention. The shrinkage rate for the casting material was negligible (listed as 0.32% after 7 days in Perry et al., 2000). The lungs were removed from the

TABLE 1. Data in this and previous studies

(a) Number of airways analyzed and body weight

Casts	Right apical	Right cardiac	Right diaphragmatic	Right intermediate	Left apical	Left diaphragmatic	Total number of airways	Body weight (g)
Rat #1	521	590	1016	304	521	743	3700	248
Rat #2	591	327	595	202	244	912	2876	299.4
Rat #3	969	583	1433	813	323	1407	5533	309.2
Rat #4	787	752	1489	508	547	1498	5586	314.6
Rat #5	819	422	1798	649	243	1353	5289	327.7
Rat #6	717	517	1578	728	436	1307	5288	317.8
Raabe et al.	445	604	1530	632	393	1198	4807	330

(b) Gravity angle at each lobe

Casts	Right apical	Right cardiac	Right diaphragmatic	Right intermediate	Left apical	Left diaphragmatic	Average gravity angle
Rat #1	99.9	83.3	91.9	89.9	95.7	90.5	91.7
Rat #2	93.8	90.7	93.9	90.2	90.0	81.4	89.0
Rat #3	94.8	92.0	89.3	96.3	93.8	89.9	92.0
Rat #4	95.9	90.0	89.3	93.9	98.9	87.4	91.2
Rat #5	96.3	91.2	88.1	95.1	95.2	86.5	90.4
Rat #6	97.1	85.47	88.9	88.3	89.9	81.3	87.9
Raabe et al.	80.6	79.4	90.5	82.4	82.5	94.3	87.64

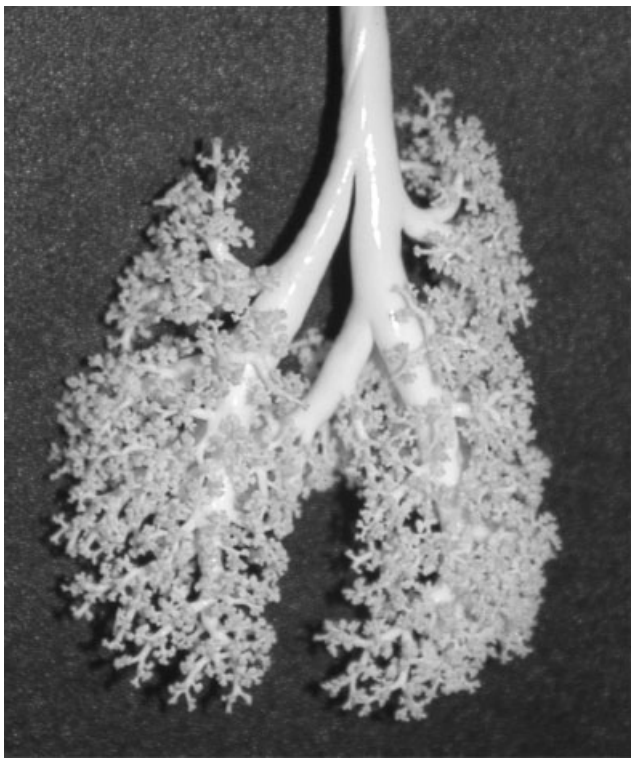

Fig. 1. Lung cast from rat #5.

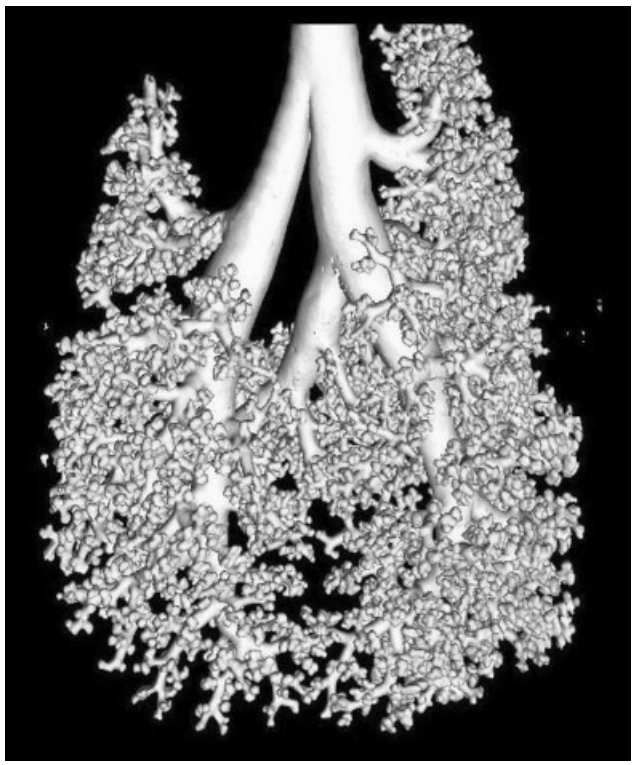

Fig. 2. A 3D reconstructed CT image from rat #5.

negative pressure chamber and exposed to air to dry the silicone. There was no detectable expansion or shrinkage with depressurization. Twenty-four hours later, the lungs were placed in bleach (6% sodium hypochloride; Clorox, Oakland, CA) to dissolve the lung tissue. Bleach dissolved all tissue but did not affect the silicone cast of the airway tree (Fig. 1).

Acquisition of Voxel Data

The rat lung casts were imaged using a commercially available micro CT scanner, MicroCAT II (Siemens, Knoxville, TN) in high resolution mode with a 0.5-mm aluminum filter. To prevent motion artifact, the cast was imaged in a plastic tray. Three hundred sixty projections were acquired during a full rotation around the cast with the following scan parameters: 80 kVp, 500 μA, 1,250 ms per frame and 30 calibration images (bright- and darkfields). Total scan time for the two bed position acquisition was 25 min. The image was reconstructed using the Feldkamp reconstruction algorithm as a 768 × 768 × 1,000 array with corresponding voxel size of 0.053 mm × 0.053 mm × 0.053 mm (Fig. 2). Image resolution was 43 microns. As a test of the dependence of the results on voxel size, one cast was scanned at a resolution of 0.026 mm × 0.026 mm × 0.026 mm but the differences were not significant; the difference in diameter, length and rotation angle (angle between successive bifurcations) as a function of generation number was 6%, 9%, and 7%, averaged over each generation and difference in branching angle as a function of diameter was 6%, averaged over each diameter range.

Flexible Bifurcation Model

A flexible bifurcation model is used to extract key airway geometric data from the CT images. The general construction of the bifurcation model follows that of Heistracher and Hofmann (1995). In this study, Heistracher's model was modified so as that carinal ridge starting point is shifted toward the smaller daughter branch (http://mae.ucdavis.edu/wexler/lungs/bifurc.htm), which prevents distortion in a very asymmetric bifurcation as well as is closer to real airway shape. By varying the combination of geometry parameters such as parent diameter, daughter diameter, and bifurcation angle, various bifurcation shapes can be duplicated.

Characterization of Pulmonary Architecture Using Optimization Method

Using the flexible bifurcation model, a parameter set that minimizes the distance between the airway CT image and the bifurcation model is searched at each bifurcation. Figure 3 illustrates this technique. Along normal vectors that originate from the bifurcation model surface, distances between the bifurcation model surface and that of the airway image are calculated. The average value of these distances is a measure of deviation between image and model. This average distance decreases and eventually becomes very small as the shape and location of bifurcation model get close to that of the image. Therefore by searching for a parameter set that minimizes average distance, we identify important

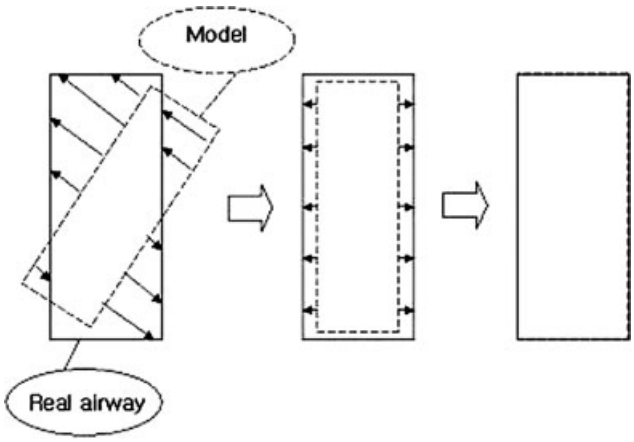

Fig. 3. Schematic of pulmonary characterization algorithm.

geometric parameters, position and rotation of the airway, in addition to a measure of the quality of the fit between the model and image.

This optimization problem is of large scale and one where a desired global minimum is hidden among many, poor, local minima. The simulated annealing method, known to be suitable for this kind of problem, is adopted to find the best fit. Simulated annealing minimizes an objective function, which in the current study is defined as the average distance between the model and image. Objective function, F, is defined by Equation 1 where the Np, Nt, Nl, and Nr are the number of normal vectors that were originated from parent branch, transition zone, left daughter, and right daughter branches, respectively. ΔE_i is the error at the ith normal vector and R_p, R_l, and R_r are branch radius of parent, left daughter, and right daughter. Relative error instead of absolute error is used because all errors should be weighted equivalently whether measured at parent branch or daughter branch; for example if an absolute error, ΔE_i, is very small but is large compared with the corresponding branch radius, it must be evaluated as large error.

$$F = \frac{\sum_i^{Np} (\Delta E_i/R_p)^2}{Np} + \frac{\sum_i^{Nt} (\Delta E_i/R_p)^2}{Nt} + \frac{\sum_i^{Nl} (\Delta E_i/R_l)^2}{Nl} + \frac{\sum_i^{NR} (\Delta E_i/R_r)^2}{NR} \quad (1)$$

A major advantage of simulated annealing over local optimization methods is an ability to avoid being

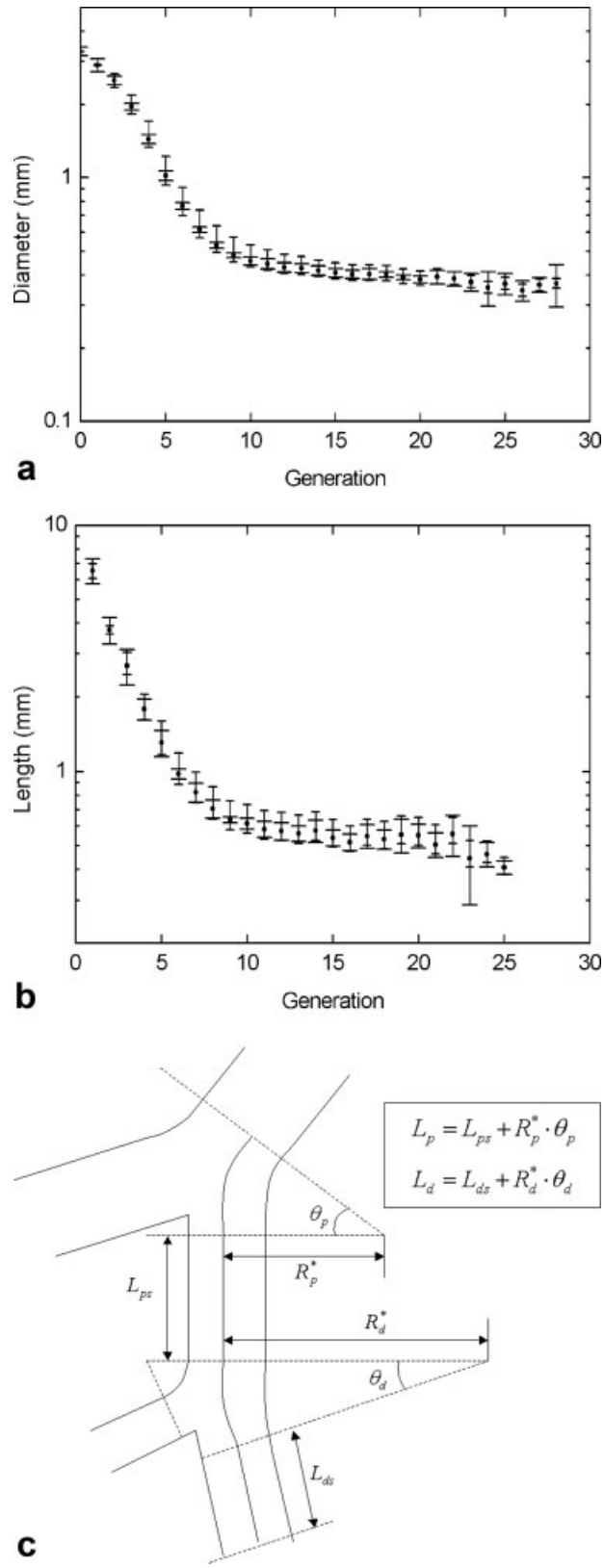

Fig. 4. **a,b:** Diameter (a) and length (b) with generation number. Wider error bars indicate intersubject variance while narrower ones indicate intrasubject variance for these figures and all subsequent ones. For intrasubject variance, upper variance and lower variance were plotted separately. **c:** Length was calculated by summing straight section of the airway and curved section in bifurcation region.

TABLE 2. Statistics of airway diameter for each generation[a]

Generation	Min (mm)	Mean (mm)	Max (mm)	SD1 (mm)	SD2 (mm)
0	3.13	3.30	3.48		0.134
1	2.53	2.90	3.33	0.0196	0.177
2	1.64	2.51	3.43	0.161	0.106
3	1.02	1.96	3.59	0.175	0.0612
4	0.441	1.44	3.40	0.167	0.0592
5	0.308	1.02	3.25	0.140	0.0447
6	0.200	0.764	2.77	0.105	0.0234
7	0.231	0.612	2.63	0.0796	0.0152
8	0.196	0.528	2.32	0.0642	0.0147
9	0.181	0.481	2.52	0.0546	0.0113
10	0.170	0.457	2.82	0.0485	0.0171
11	0.165	0.444	2.02	0.0435	0.0225
12	0.170	0.430	2.10	0.0398	0.0189
13	0.170	0.426	1.98	0.0373	0.0177
14	0.158	0.417	1.78	0.0339	0.0188
15	0.172	0.408	1.60	0.0316	0.0163
16	0.166	0.403	1.52	0.0304	0.0169
17	0.162	0.404	1.38	0.0305	0.0209
18	0.178	0.401	1.24	0.0294	0.0110
19	0.164	0.391	1.01	0.0272	0.00926
20	0.172	0.383	0.968	0.0261	0.0133
21	0.174	0.392	1.08	0.0282	0.0256
22	0.173	0.386	0.850	0.0238	0.0251
23	0.185	0.374	0.802	0.0216	0.0306
24	0.175	0.355	0.937	0.0197	0.0575
25	0.172	0.368	0.951	0.0219	0.0364
26	0.168	0.345	0.667	0.0196	0.0334
27	0.182	0.364	0.562	0.0196	0.0251
28	0.198	0.368	0.566	0.0158	0.0729

[a]min, smallest diameter; mean, mean diameter; max, largest diameter; SD1, intrasubject standard deviation; SD2, intersubject standard deviation.

trapped at local minima. Details on simulated annealing method are presented by Corana et al. (1987).

In the present study, optimization is divided into three steps. In the first step, a cylinder with variable diameter but fixed length is fit to the parent airway to find its rough position, orientation and diameter. In the second step, the distance from the center of airway to airway edge is measured along the axial direction that was obtained in the first step. This distance (l_{dis}) will abruptly increase near the bifurcation. We assumed that the position where $|l_{dis}–R_p|$ is larger than $0.5\dot{s}R_p$ is near the bifurcation (R_p is the cylinder radius obtained in the first step). This estimated position is used as the bound of L_p in the third step. In the third step, identification of all parameters is conducted under reasonable bounds that were determined based on lung airway anatomy. Lower and upper bounds for each parameter are as follows:

$$L_p < \min(1.5 \cdot L_{bd}, 20 \cdot R_p)$$
$$0.2 \cdot R_p < R_d < 1.2 \cdot R_p$$
$$1^\circ < \alpha_1, \alpha_2 < 90^\circ$$
$$0.1 \cdot R_p < R^* < 30 \cdot R_p$$

L_{bd} is bifurcation position that was estimated in the second step, R_p and R_d are radii of parent and daughter branch, respectively, R^* is offspring radius of curvature, and α is acute angle between the direction of the parent airway and the directions of the daughter airways (α_1 for major daughter and α_2 for minor daughter). These three steps, fitting cylinder, estimating L_{bd}, and full optimization, are iteratively applied down to the airway tree. The bifurcation model used to identify geometry information from the image has a curved portion so it can handle curved airways. In addition, if an airway is severely curved, the program repeats the first step in the fitting process until it finds reasonable fit in the third step. Our program reports average diameter when the airway diameter changes along its length.

The casts were laid down in the plastic tray during each scan deforming the airways. To investigate this effect, we have compared a scan lying down with one scanned hanging (Rat #2). Cast deformation seems to affect rotation angle the most especially at generations proximal to 6. Difference in diameter, length and rotation angle as a function of generation number was 7%, 12%, and 14%, averaged over generations. Difference in branching angle as a function of diameter was 7%, averaged over each diameter range. Although both postures will cause deformation, lying down may decrease the artifact of gravity because distal airways touching the tray will support the whole cast while in a hanging position, more airways will sag (Fig. 1).

Voxel size of the image data determines the limit of morphometric analysis using image data. It is reasonable to assume that approximately a half voxel would be the best accuracy that the computer algorithm can achieve, so airways with radius twice the voxel size will cause unavoidable relative error of 12.5 % (absolute

error divided by diameter). We did not analyze airways with radius smaller than two voxels (approximately 0.1 mm) or relative error larger than 0.125.

RESULTS

Generation-Based Analysis

In Weibel's (1963) well-known and much used model, the airways are classified by generations, labeling the trachea 0 and increasing by 1 at each bifurcation. Figure 4 shows airway diameter and length by generation (data for diameter are also presented in Table 2). Airway diameter was 3.3 mm at the trachea and decreased to 0.35 mm in distal generations. Airway length decreased similarly to diameter. In general, both inter- and intra-subject variances were small compared with the average diameter or length. Diameter, $d(z)$, fit an exponential function as in Weibel (1963) but length, $L(z)$, fit a modified exponential function for $z < 9$, where z is generation number. Figure 4c shows bifurcation point of the parent and daughter and how the airway length is measured.

$$d(z) = 3.3 \cdot \exp(-0.209 \cdot z): \quad 0 \le z < 9 \tag{2a}$$

$$d(z) = 0.48 \cdot \exp(-0.0186 \cdot (z-9)): \quad z \ge 9 \tag{2b}$$

$$L(z) = 38 \cdot \exp(-1.752 \cdot z^{0.4}): \quad 0 \le z < 9 \tag{3a}$$

$$L(z) = 0.637 \cdot \exp(-0.0207 \cdot (z-9)): \quad z \ge 9 \tag{3b}$$

The angle between successive bifurcations is termed the rotation angle (Sauret et al., 2002). For instance, if two successive bifurcations are both in the same plane, the rotation angle is 0 degrees. If, on the other hand, two successive bifurcations are orthogonal to each other, the rotation angle is 90 degrees. These are the two limiting cases—that is, the minimum value for rotation angle is zero and the maximum is 90. Rotation angle has been infrequently reported because it is very difficult to extract this data directly from the airways or their casts manually. The only data that we are aware of were obtained by tomographic imaging (Sauret et al., 2002), similar to the techniques used in the current work. Rotation angle is an important geometric parameter, because it will affect pressure drop in proximal airways (where the Reynolds number is higher) and will change particle deposition/transport patterns (Comer et al., 2000; Lee et al., 2000). In addition rotation angle is useful for construction of 3D lung model or lung growth simulations (Kitaoka et al., 1999; Tebockhorst et al., 2007).

Figure 5a shows that rotation angles are smaller in the first several generations indicating that the first few airways bifurcate rather in-plane while in subsequent generations they are more out-of-plane. Intersubject variance was very small in generations between 6 and 19.

In cases where the distribution of a variable is close to normal, average and standard deviation are enough to describe the variable. However, rotation angle was far from normally distributed. Figure 5b shows that most bifurcations are rotated close to 90 degrees from the parent bifurcation even though the average rotation angle was close to 55 degrees. Of interest, for airways smaller than 2 mm in diameter, the distribution of rotation angle was very similar between casts, indicating that, except for the proximal two or three generations, rotation angle can be represented by a single distribution function. The distribution of rotation angles, averaged for these six subjects, is given by:

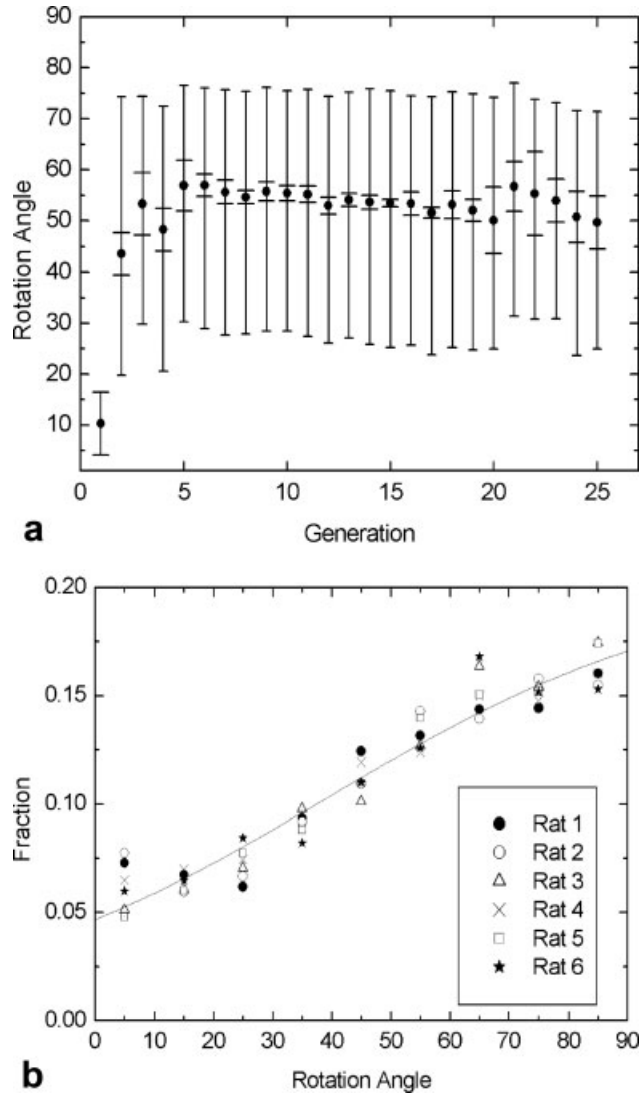

Fig. 5. **a:** Rotation angle with generation number. Inter- and intra-subject variability as in Figure 4. **b:** Distribution of rotation angle for airway diameter smaller than 2 mm. Fraction is the number of airways in an interval divided by total number of airways.

$$f(\theta) = \frac{0.0604}{0.2936 + \exp(-0.0313 \cdot \theta)} \tag{4}$$

Table 1b shows gravity angle for each lobe. Gravity angle from our data was slightly larger than Raabe et al. (1976). There was no appreciable difference in gravity angle between lobes. Cumulative distribution of the gravity angles was similar to the Koblinger and Hoffmann (1988) analysis of the data by Raabe et al.

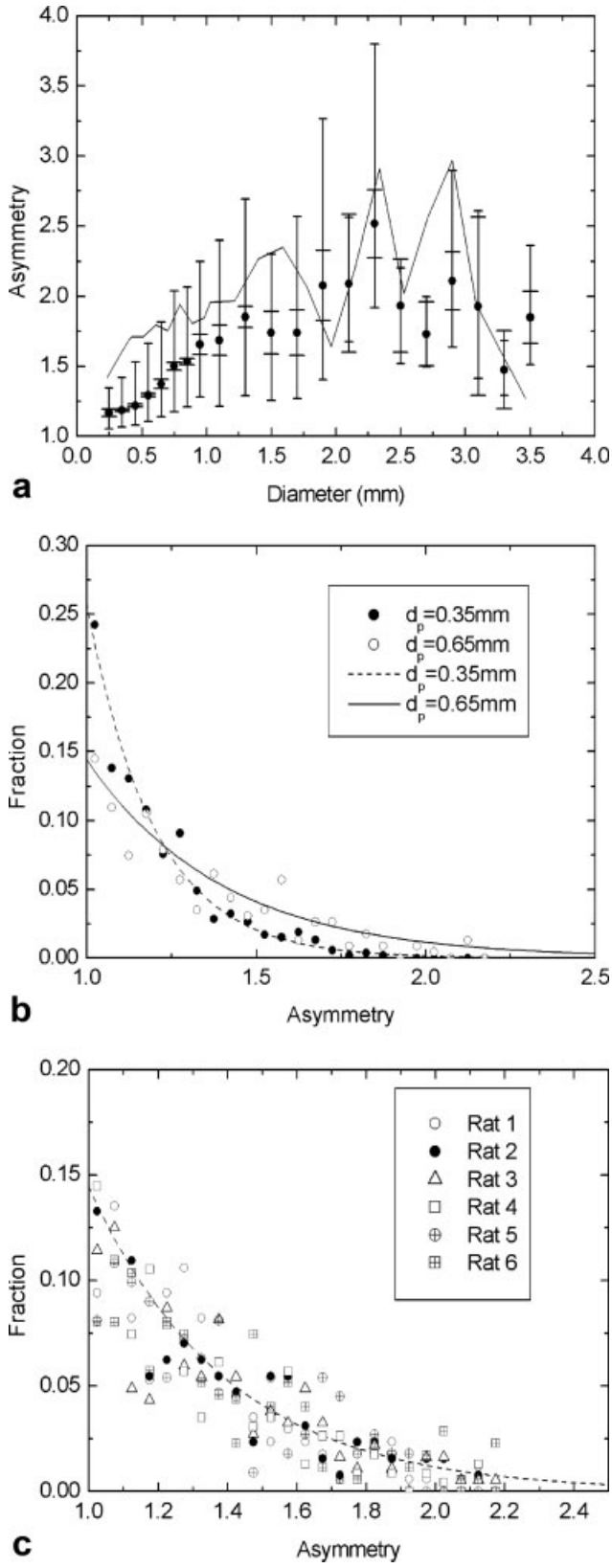

Fig. 6. **a:** Ratio of major to minor daughter diameter (asymmetry) as a function of parent diameter. The line is Raabe et al. (1976). For diameter-based analysis, data are grouped into 0.1 mm bins for diameters smaller than 1.0 mm and 0.2 mm bins for diameters larger than 1.0 mm. **b:** Distribution of asymmetry for airways smaller than 0.9 mm (Rat #4). Average asymmetry for d_p = 0.35 mm and 0.65 mm was 1.186 and 1.374, respectively. **c:** Distribution of asymmetry is similar between subjects. The figure shows an example for the, $0.6 \leq d_p \leq 0.7$ mm interval.

(1976); the most airways had gravity angle approximately 90 degrees and gravity angles near 0 degrees or 180 degrees were rare.

Diameter-Based Analysis

For some geometric parameters, diameter-based analysis (Phillips and Kaye, 1995) is more useful than generation-based analysis to describe monopodial branching patterns in rat airways. Asymmetric branching features such as ratio of daughter diameters and ratio of daughter branching angles are essential for modeling monopodial architecture.

Figure 6a shows the ratio of major daughter diameter to minor daughter diameter (asymmetry) as a function of parent diameter. Although asymmetry of larger, proximal airways is quite scattered, both inter- and intrasubject variability decreases in distal airways coincident with branching becoming more symmetric.

As was rotation angle, asymmetry in diameter was also far from normally distributed especially for airways smaller than 0.9 mm in diameter. While distribution of asymmetry was rather random for airways larger than 0.95 mm in diameter, distribution had a clear pattern for airways smaller than 0.9 mm (Fig. 6b). Because for these distal airways intersubject variability was small (Fig. 6c), the distribution for airways smaller than 0.9 mm could be fit with:

$$f(x) = a \cdot \exp(-b \cdot (x - 1)) \tag{5}$$

where $a = -0.51 \cdot d_p + 0.475$, $b = -11 \cdot d_p + 10.37$, and *f(x)* expresses the fraction of airways with asymmetry x and parent airway diameter d_p [mm].

Figure 7a shows branching angle as a function of parent diameter. Although intrasubject variance was huge, average branching angle was very regular and close to 30 degrees. Intersubject variance was smaller for small airways than for large airways. However, intrasubject variance was large both for small airways and large airways, which indicates that contrary to asymmetry in diameter, branching angle is very irregular in all diameter ranges. Figure 7a does not show any correlation between branching angle and parent diameter.

Correlation Between Geometry Parameters

Figure 7b shows correlation between branching angle and ratio of daughter to parent diameter (d/d_p). Branching angle increased almost linearly with d/d_p indicating that minor daughters turn more sharply than major ones.

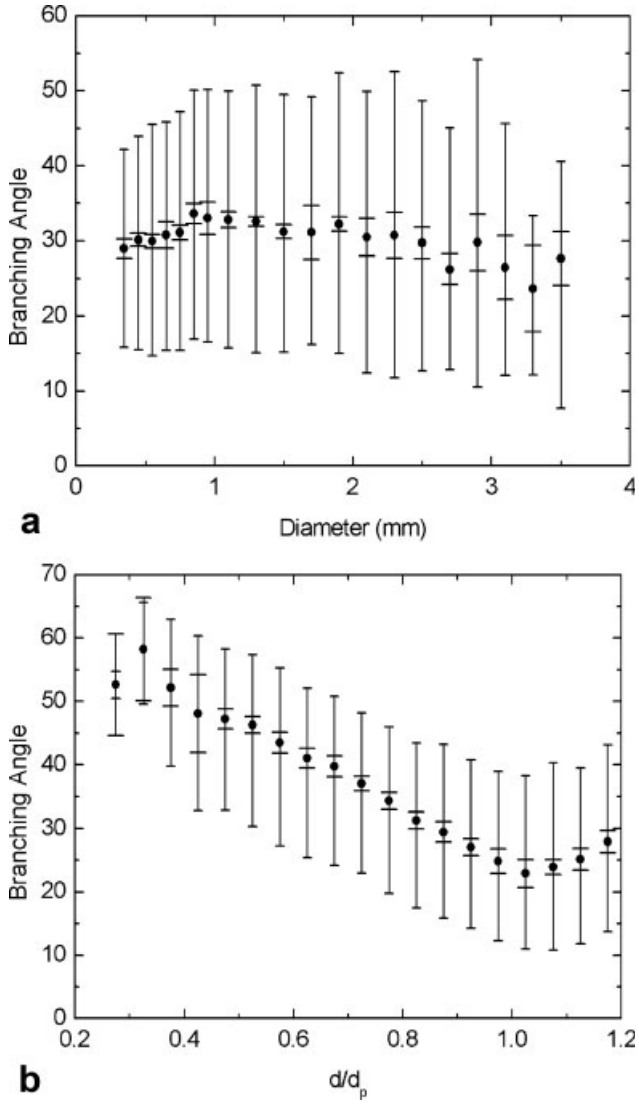

Fig. 7. **a:** Branching angle as a function of parent diameter. **b:** Correlation between branching angle and ratio of airway diameter to its parent diameter.

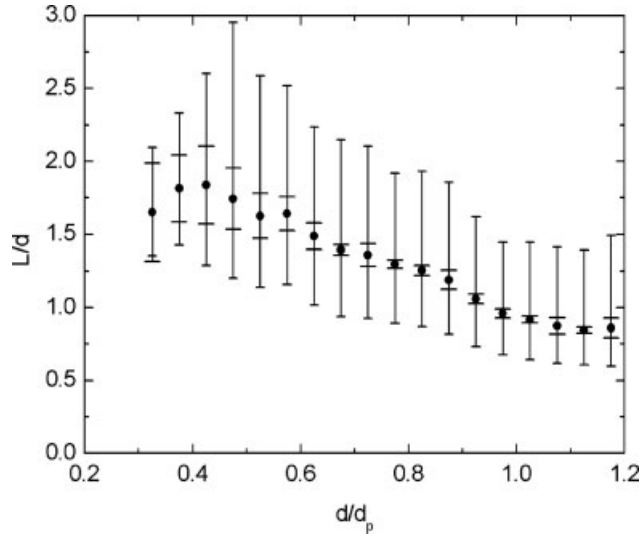

Fig. 8. Correlation between length to diameter ratio and ratio of airway diameter to its parent diameter.

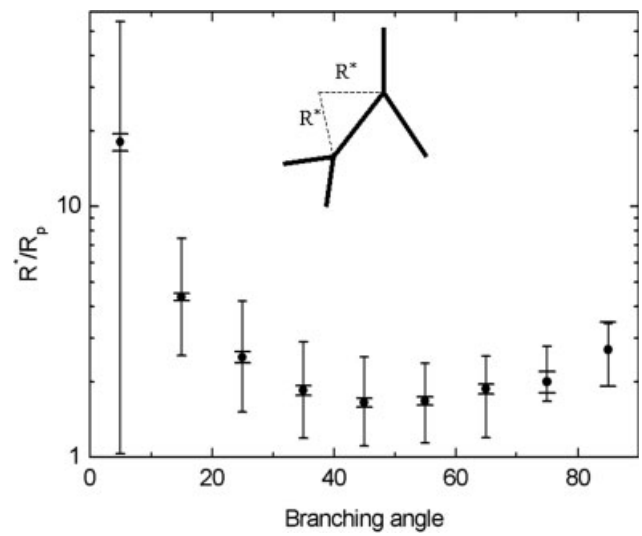

Fig. 9. Correlation between radius of curvature of the daughter airway toroid (R^*) and branching angle. R_p is parent diameter.

Length–diameter ratio also shows a correlation with d/d_p (Fig. 8). Length to diameter ratio was appreciably larger for small d/d_p indicating that length, compared to diameter, of strictly minor daughter is larger than that of major daughter. Previous studies (Phalen et al., 1978; Phillips and Kaye, 1995) show that the length to diameter ratio of the minor daughter is clearly larger than that of the major one, which agrees with our results (Fig. 8).

The daughter airway radius of curvature (R^*) is difficult to measure accurately because of the difficulty distinguishing between curved and straight portions of the airway. In this study, R^* is estimated from the bifurcation point of parent and daughter airways (Fig. 9). R^*/R_p was very large especially for small branching angle. Of interest, R^*/R_p was smallest near branching angle 45 degrees but somewhat larger for branching angles closer to 90 degrees.

Number of Airways and Number of Generations to Reach an Airway Diameter

Table 1 shows the total number of airways analyzed in this and previous studies. Intersubject variability in the number of airways may be due to natural variation, limitations in the analysis methods or variation in the casting conditions (repeatability). As was clarified in materials and methods, we confined our analysis to airways whose radius is larger than two voxels (approximately 0.2 mm in diameter) and whose relative error is less than 0.125. These constraints may lead to increased intersubject variability in certain parameters because different overall lung size will dramatically change the

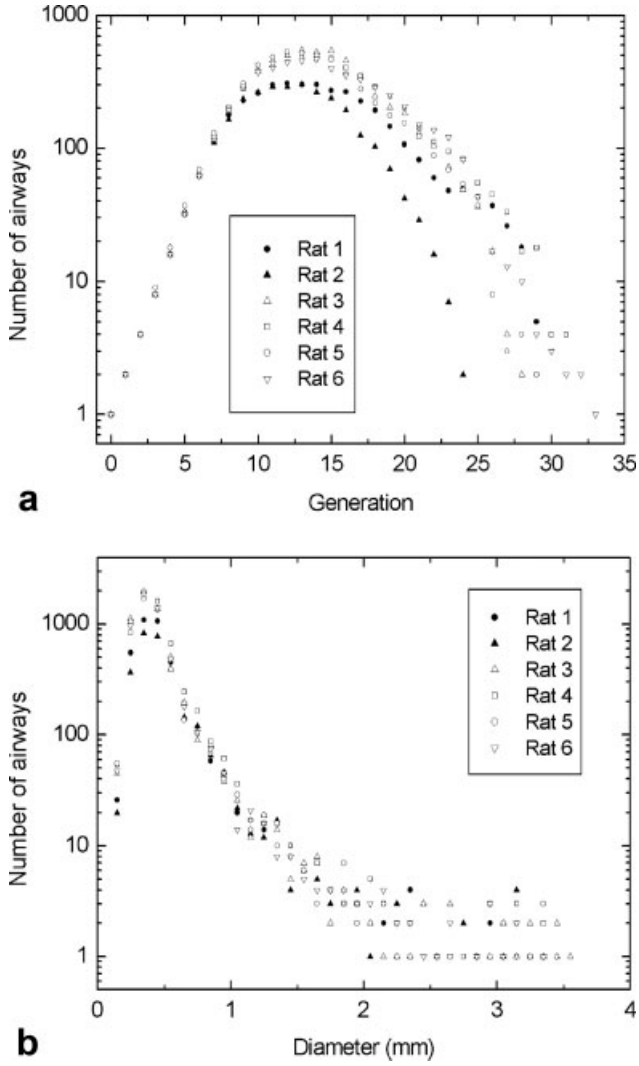

Fig. 10. **a:** Number of airways analyzed at each generation for each airway cast. **b:** Number of airways as a function of airway diameter.

TABLE 3. Number of generations (NG) to reach an airway as a function of diameter[a]

Diameter (mm)	Min	Mean	Max	SD1	SD2
0.15	8	15.93	29	4.05	0.99
0.25	6	15.33	31	4.15	0.81
0.35	5	14.17	33	4.10	0.61
0.45	4	13.86	32	4.23	0.70
0.55	4	13.63	29	4.37	0.56
0.65	4	12.81	26	4.08	0.79
0.75	4	11.74	25	3.95	0.57
0.85	4	10.56	23	3.88	0.40
0.95	4	10.00	25	3.92	0.69
1.05	3	9.88	21	3.61	1.21
1.15	3	9.31	17	3.49	0.94
1.25	3	8.72	18	3.54	0.83
1.35	3	7.94	17	2.85	0.75
1.45	3	7.22	14	2.73	0.90
1.55	3	7.34	16	3.05	1.14
1.65	2	7.67	15	3.18	1.17
1.75	2	6.75	14	1.78	3.20
1.85	2	7.76	13	2.27	1.62
1.95	2	7.68	13	2.76	1.87
2.05	3	6.67	12	1.34	2.54
2.15	3	6.72	12	1.45	2.93
2.25	4	5.58	8	0.62	0.84
2.35	4	7.05	9	0.67	1.29
2.45	3	4.36	9	0.95	1.12
2.55	1	5.67	9	0.00	3.40
2.65	1	4.90	7	0.46	2.11
2.75	1	4.75	6	1.25	1.25
2.85	1	2.67	10	0.00	3.30
2.95	1	4.03	5	0.65	0.60
3.05	1	2.70	4	0.50	0.51
3.15	0	2.29	5	0.79	0.71
3.25	0	2.50	5	0.25	0.83
3.35	0	1.33	2	0.33	0.47
3.45	0	2.00	4	0.80	0.82
3.55	3	3.00	3		

[a]Data are grouped into 0.1-mm diameter bins; values in the first column indicate mean diameter for each interval. Min, smallest NG; mean, mean NG; max, largest NG; SD1, intrasubject standard deviation of NG; SD2, intersubject standard deviation of NG.

number of airways at the limits of the analysis (close to 0.2 mm). Figure 10 shows the number of airways at each generation analyzed for all subjects. Intersubject variability in the number of airways becomes significant for generations larger than 7 or for airways smaller than 0.5 mm in diameter. However, as can be seen in Figures 5b or 6c, there were not significant differences in the statistics of lung geometry between casts. Because of the potentially missed airways, average airway size could be a little different from reality especially for distal generations.

Table 3 shows the number of generations (*NG*) to reach an airway as a function of diameter range. Number of generations to reach 0.35 mm, which will be close to terminal bronchioles (Phillips and Kaye, 1995), ranges from 6 to 33, which indicates that global architecture of rat airways is highly asymmetric. Intrasubject variance of *NG* to reach around 0.35 mm is less than 1.

DISCUSSION

Figure 11 compares this and previous studies (Raabe et al., 1976; Sera et al., 2003). Our values of airway diameter vs. generation number were closest to Raabe et al. (1976), but diameter was a little larger than Raabe for distal generations. Sera et al. (2003) analyzed small airways of male Wister rats using CT images finding diameters clearly smaller than other observations (Fig. 11a).

Even considering intersubject variability, it is apparent that our measurements of asymmetry are clearly smaller than Raabe's especially for airways smaller than 1.2 mm (Fig. 6a). For one rat lung (#4), we found that improving the resolution by using half the voxel size did not cause appreciable difference in asymmetry estimates. Asymmetry variation with diameter was very similar between male and female rats in Raabe et al. (1976), which indicates gender might not be a major factor, but other studies did not report asymmetry so species differences cannot be deduced.

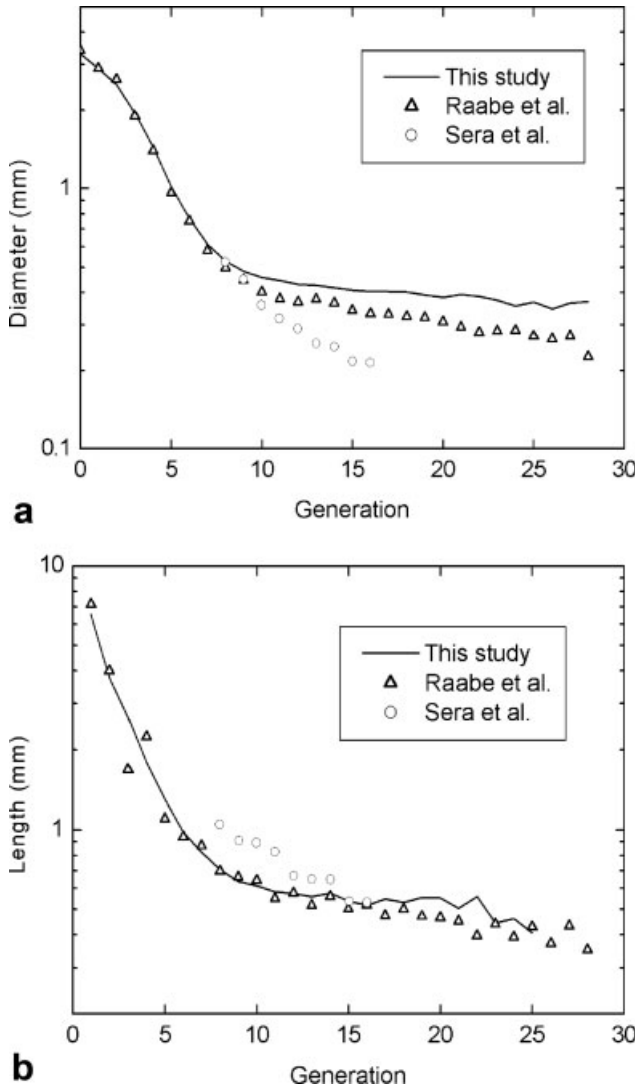

Fig. 11. Comparison to previous studies. **a:** Airway diameter by generation. **b:** Airway length by generation. While all data from Raabe et al. (1976) were combined for diameter, the data with incomplete length measurement or incomplete casting were excluded for length.

According to our study both inter- and intrasubject variance in airway size were not large compared with the variance between studies (Figs. 4a,b, 11a,b). The difference between gender was also negligible according to Raabe's data although measurements of the male rat was not complete. Airway size appears to be independent of body weight for adult rats (Table 1); no correlation was found between body weight and airway size. Therefore disagreements between studies might be caused by the different species used in the studies and different measurement techniques or airway casting conditions. For example, scans of Sera et al. (2003; body weights 300 g ± 30) were from an ex vivo preparation that is likely to have artifacts from hanging the lung while scanning, not to mention the ongoing tissue shrinkage occurring during scanning. Also, computerized and manual measurement techniques likely have uncharacterized error or bias.

Average rotation angle in rat is much smaller than that of human (Sauret et al., 2002) probably because chest shape forces rotation angles in proximal airways that fill the chest. It is interesting that rotation angle is smaller in the first several generations compared with succeeding ones, which indicates that airways bifurcate rather in-plane before dividing into lobes and bifurcations inside lobes are more out-of-plane.

Koblinger and Hofmann (1985) tallied diameters and lengths into seven equiprobability classes for each generation without out presenting any correlations with other parameters. Figure 8 shows that length to diameter ratio is correlated with d/d_p. Furthermore, this correlation presents a simple method for selecting airway length in stochastic airway models. Correlation between branching angle and d/d_p (Fig. 7b) will also be useful for selecting branching angle in such models. These two correlations indicate typical characteristics of rat monopodial architecture, that is, length compared to diameter is small along the main branch and side branches bend with large branching angle.

Figures 5b and 6b suggest that distribution of parameters should be taken into account in stochastic lung models; modeling airways using only mean value and standard deviation can distort characteristics of asymmetry and rotation angle. The distribution of asymmetry for these six rats was very similar to each other especially for diameters smaller than 0.8 mm (Fig. 6b). Distribution of rotation angle was similar as well for airways smaller than 2 mm (or generation larger than 3). Number of generations to reach near terminal bronchioles was very similar between subjects (Table 3). These similarities between subjects indicate that airways have a typical branching pattern not only on average (e.g., Fig. 4) but also in detail.

On the whole intersubject variability was small both in generation- and diameter-based analysis. Variation of airway size with generation number (Fig. 4) indicates that global features of airway architecture are similar between subjects. Variations of asymmetry, branching angle and rotation angle shows that more detailed features are similar between subjects. Furthermore, as discussed above, distribution functions of asymmetry and rotation angle were very similar between subjects. Overall, these patterns in airway architecture indicate that models based on only several rats can be representative if a sufficient number of airways are analyzed.

ACKNOWLEDGMENTS

Although the research described in the article has been funded in part by the United States Environmental Protection Agency to the University of California, Davis, it has not been subject to the Agency's required peer and policy review and, therefore, does not necessarily reflect the views of the Agency and no official endorsement should be inferred. Research described in this article was supported in part by Philip Morris USA Inc. and Philip Morris International.

LITERATURE CITED

Comer JK, Kleinstreuer C, Hyun S, Kim CS. 2000. Aerosol transport and deposition in sequentially bifurcating airways. J Biomed Eng 122:152–158.

Corana A, Marchesi M, Martini C, Ridella S. 1987. Minimizing multimodal functions of continuous variables with the "simulated annealing" algorithm. ACM Trans Math Software 13:262–280.

Dockery D, Pope C. 1994. Acute respiratory effects of particulate pollution. Annu Rev Public Health 15:107–132.

Gauderman WJ, McConnell R, Gilliland F, London S, Thomas D, Avol E, Vora H, Berhane K, Rappaport EB, Lurmann F, Margolis HG, Peters J. 2000. Association between air pollution and lung function growth in southern California children. Am J Respir Crit Care Med 162:1383–1390.

Heistracher T, Hofmann W. 1995. Physiologically realistic models of bronchial airway birfurcations. J Aerosol Sci 26:497–509.

Holgate ST, Samet JM, Koren HS, Maynard RL. 1999. Air pollution and health. San Diego: Academic Press.

Kitaoka H, Takaki R, Suki B. 1999. A three-dimensional model of the human airway tree. J Appl Physiol 87:2207–2217.

Koblinger L, Hofmann W. 1985. Analysis of human morphometric data for stochastic aerosol deposition calculations. Phys Med Biol 30:541–556.

Koblinger L, Hofmann W. 1988. Stochastic morphological model of the rat lung. Anat Rec 221:533–539.

Lee JW, Lee DY, Kim WS. 2000. Dispersion of an aerosol bolus in a double bifurcation. J Aerosol Sci 31:491–505.

Mariassy AT, Sielczak MW, McCray MN, Abraham WM, Wanner A. 1989. Effects of ozone on lamb tracheal mucosa: quantitative glycoconjugate histochemistry. Am J Pathol 135:871–879.

Mariassy AT, Abraham WM, Phipps RJ, Sielczak MW, Wanner A. 1990. Effect of ozone on the postnatal development of lamb mucociliary apparatus. J Appl Physiol 68:2504–2510.

Perry SF, Purohit AM, Boser S, Mitchell I, Green FH. 2000. Bronchial casts of human lungs using negative pressure injection. Exp Lung Res 26:27–39.

Phalen RF, Yeh HC, Schum M, Raabe OG. 1978. Application of an idealized model to morphometry of the mammalian tracheobronchial tree. Anat Rec 190:167–176.

Phillips CG, Kaye SR. 1995. Diameter-based analysis of the bronchial geometry of four mammalian bronchial trees. Respir Physiol 102:303–316.

Raabe OG, Yeh HC, Schum GM, Phalen RF. 1976. Tracheobronchial geometry: human, dog, rat, hamster. LF-53. Albuquerque, NM: Lovelace Foundation for Medical Education and Research.

Sauret V, Halson RM, Brown IW, Fleming JS, Bailey AG. 2002. Study of the three-dimensional geometry of the central conducting airways in man using computed tomographic (CT) images. J Anat 200:123–134.

Sera T, Fujioka H, Yokota H, Makinouchi A, Himeno R, Schroter RC, Tanishita K. 2003. Three-dimensional visualization and morphometry of small airways from microfocal X-ray computed tomography. J Biomech 36:1587–1594.

Tawhai MH, Hunter P, Tschirren J, Reinhardt J, McLennan G, Hoffman EA. 2004. CT-based geometry analysis and finite element models of the human and ovine bronchial tree. J Appl Physiol 97:2310–2321.

Tebockhorst S, Lee DY, Wexler AS, Oldham MJ. 2007. Interaction of epithelium with mesenchyme affects global features of lung architecture: a computer model of development. J Appl Physiol 102:294–305.

Weibel ER. 1963. Morphometry of the human lung. New York: Academic Press.

Yeh HC, Schum GM, Duggan MT. 1979. Anatomic models of the tracheobronchial and pulmonary regions of the rat. Anat Rec 195: 483–492.